Jülich Solar Power Tower – System Behavior During Downtime

Torsten Baumann[1, a)], Felix Göhring[1, b)], Hannes Stadler[1,c)] and Till Doerbeck[2,d)]

[1]*German Aerospace Center (DLR), Institute of Solar Research, Karl-Heinz-Beckurts-Str. 13, 52428 Jülich, Germany*
[2]*Kraftanlagen München GmbH, Solar Technology/Energy and Environment Technology, Ridlerstraße 31c, 80339 München, Germany*

[a)]Corresponding author: torsten.baumann@dlr.de
[b)]felix.goehring@dlr.de
[c)]hannes.stadler@dlr.de
[d)]till.doerbeck@kraftanlagen.com

Abstract. At the Jülich Solar Power Tower, two new shut-off dampers have been installed in the hot air piping system in order to reduce thermal losses during downtime of the plant. The thermodynamic behavior of the thermal energy storage and the steam boiler has been investigated with respect to heat losses after shut-down of the plant. Also, the change of temperature and the pressure drop at both shut-off dampers during downtime has been analyzed. Results show that for the storage, a reduction of thermal losses can be achieved by closing the damper overnight. Regarding the steam boiler, no improvements on heat losses were observed. If only two of the four storage chambers have been charged during operation, heat transfer between the chambers is observed after shut-down. It is concluded that natural convection is not the main source of thermal overnight losses, however, it can be lowered thanks to the dampers . Heat conduction and convectional heat transfer at the surfaces also contribute to the decrease of thermal energy, which can be lowered by thicker insulation layers in the future.

INTRODUCTION

The Jülich Solar Power Tower is Germany's first and only solar tower power plant for experimental and demonstration purposes applying an open volumetric receiver technology and is described in [1] and [2] in more detail. During solar operation, ambient air is sucked in and is being heated by a solar heated ceramic structure of the receiver. Subsequently, the hot air (up to 700°C) flows either through the thermal energy storage (TES) or through the steam boiler. A schematic of the plant is shown in Fig. 1.

The TES is a regenerator heat storage type with a ceramic honeycomb structure as sensible storage material. The plant's steam generator is a shell boiler with the hot air running through tubes and water in the shell.

During power plant operation, the hot air runs the steam generator, which in turn generates steam in order to run a Rankine cycle. Part of the hot air is used to simultaneously charge the TES during solar operation, e.g. if excess radiation is available. For a commercial CSP plant, the storage is usually fully charged at daytime and subsequently discharged in the evening or night time in order to keep the steam boiler running. The steam boiler runs at operation pressure before the plant is shut-down each day. If the storage is not discharged during operation (e.g. due to a low energy demand or due to test reasons like in this case), the system is shut down in a high thermodynamic state. This state can be favorable for a quick start-up of the system the next morning, since theoretically no heat-up phase is necessary. In practice, not the full thermal energy is available after overnight standstill due to thermal losses.
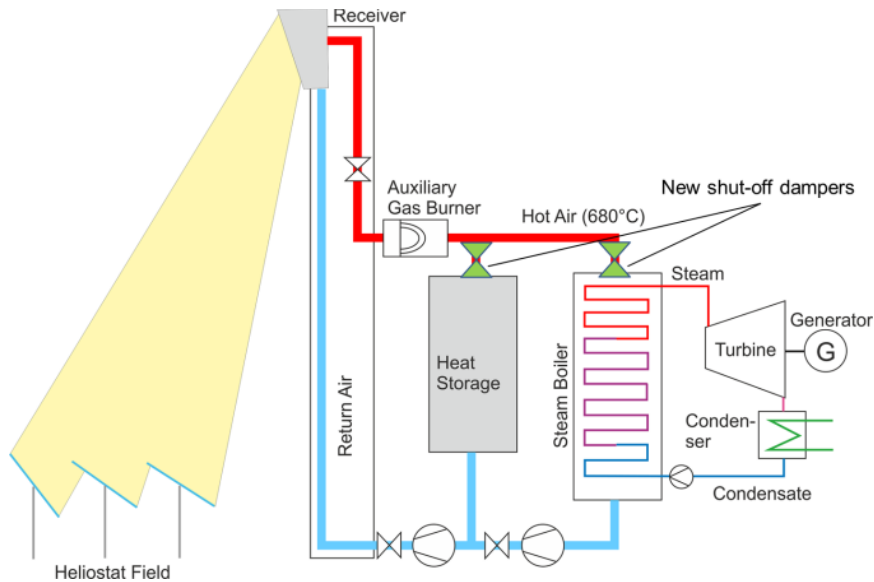
**FIGURE 1.** Schematic of the Jülich Solar Power Tower with the two new shut-off dampers

Internal studies have shown that a certain amount of heat is lost overnight presumably due to convectional heat losses. Since the air loop of the plant is not a fully closable system, convection is induced by the temperature difference to the ambient. This in turn leads to a decreasing temperature in the storage and a decreasing pressure in the steam boiler. In order to overcome the convectional losses of the air piping system, two shut-off dampers had been installed: one between the air inlet, which is the receiver, and the TES, and another between the air inlet and the steam generator. The position of both dampers is shown in Fig. 1. Both dampers should be shut close after system shut-down in order to keep the thermal energy inside the storage and the steam boiler, respectively. This study focuses on how this effort contributes to the reduction of thermal losses and the characterization of both dampers. The transient local temperature and pressure loss at each damper is analyzed as well as the temperatures inside the storage and the steam pressure of the steam boiler.

EXPERIMENTAL SETUP

The TES consists of four equally sized chambers, each virtually separated into eight levels. The chambers can be charged and discharged independently. All chambers of the storage are equipped with 24 thermocouples, three of them in each level. These thermocouples will be applied in order to account for the local temperature changes in each chamber over standstill time.

In order to quantify the thermal state of the boiler, the steam pressure is taken into account. Since the pressure of the steam directly depends on the steam temperature, the pressure represents the enthalpy of the steam.

Additionally, the temperature and the pressure loss behavior at the new dampers will be characterized. To that end, thermocouples and pressure transducers have been installed at each inlet and outlet of the two shut-off valves. Some of the measurement sensors were already pre-installed, some others (e.g. all of the pressure sensors) had to be retrofittet for this campaign. The transient behavior of temperature and pressure will be derived from the unsteady state directly after switching off the system. The pressure loss measurement also allows for the determination of the pressure loss coefficient from different steady state operations.
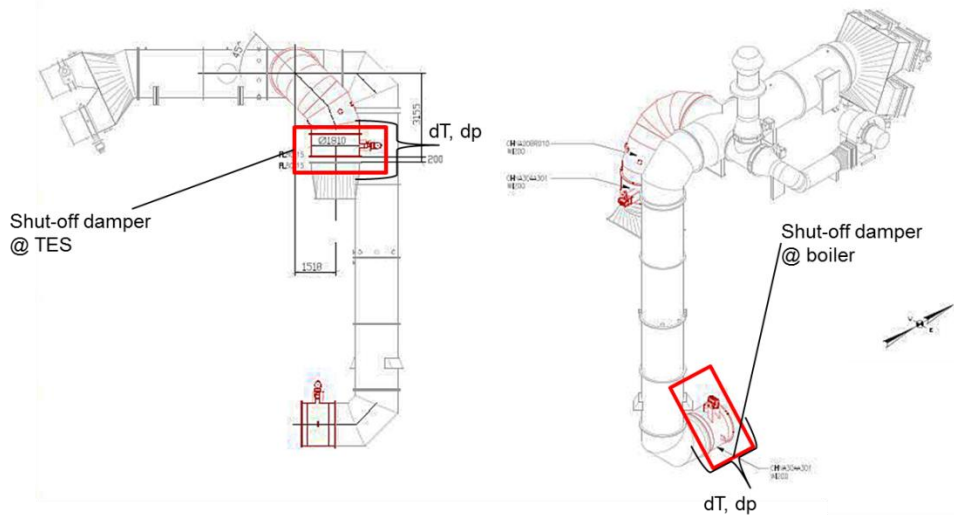
FIGURE 2. Hot air piping system from the receiver to the storage and the steam boiler with the new shut-off dampers

In order to achieve controllable and constant temperatures in the air loop for these tests, a gas burner which is installed directly behind the air inlet (see Fig. 1.) is used to heat up the incoming air from the receiver. Thus, no solar operation is applied for the experiments. This allows for constant temperatures up to 600°C at the air inlet with mass flow rates between 5 kg/s and 10 kg/s during operation. The data for unsteady behavior are recorded usually for 12 h directly after shut-down for different system configurations are summarized in table 1. At shut-down, all valves of the piping system are being closed (partially excluding the both new dampers) and the blower is shut off. As can be seen from the table, each configuration has been run with both dampers closed and opened as well. The "open" cases represent a system without the new shut-off dampers. The boiler was set to a pressure of approx. 20 bars before shut-down for each case. The storage was charged with approx. 600°C for all four chambers or only two chambers, respectively. If only two chambers have been charged during operation, the other two have been left with their current temperature. They still may remain warm from former experiments, although the temperature is noted as 20°C in table 1. All experiments have been carried out in October 2015, with ambient temperatures between 7°C and 15°C.

TABLE 1. Parameters for the test campaign; all values are target temperatures and pressures, respectively

| $T_{Storage}$ [°C]	p_{Boiler} [bar]	New dampers	Inventory dampers
600	20	closed	closed
600	20	open	closed
600/20	20	closed	closed
600/20	20	open	closed

RESULTS AND DISCUSSION

In this section, firstly, the overnight thermodynamic behavior of the storage and the steam generator will be presented. Additionally, the unsteady progress of temperature and the pressure at each damper will be looked at.

Thermodynamic behavior of TES

The progress of the mean TES temperature versus standstill time is shown in Fig. 3 for all chambers fully loaded with the damper at the storage left open, Fig. 4 shows the same diagram with the damper closed. Both figures show a decrease of the mean temperature within 12 h. For the closed damper case, the cooling rate is somewhat lower than for the open damper case: The linear cooling rates for the first and the second case are 1.64 K/h and 1.51 K/h, respectively. The difference in cooling rates represents a reduction of thermal losses of 8 % if the shut-off damper at the TES is closed.

In order to analyze the temperature progress inside the storage more closely, the local temperatures at each level of the four chambers are plotted over the storage height at both shut-down and before restart in Fig. 5 and Fig. 6. All four chambers exhibit the same temperature profiles. It should be noted that the temperature is not equally distributed in each chamber: the lower levels exhibit significantly lower temperatures than the upper levels. This is due to technical restrictions since the air blower, which is located behind the storage, must not take temperatures higher than 200°C. To that end, the charging process of the TES is stopped as soon as the outlet temperature at the lower end of each chamber comes close to 200°C, that is why an almost linear decrease of temperature from level one to level three develops.
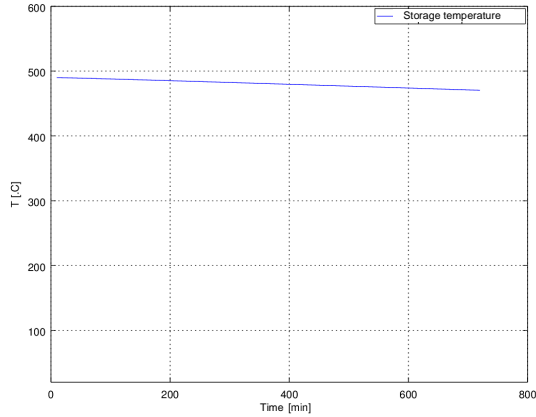

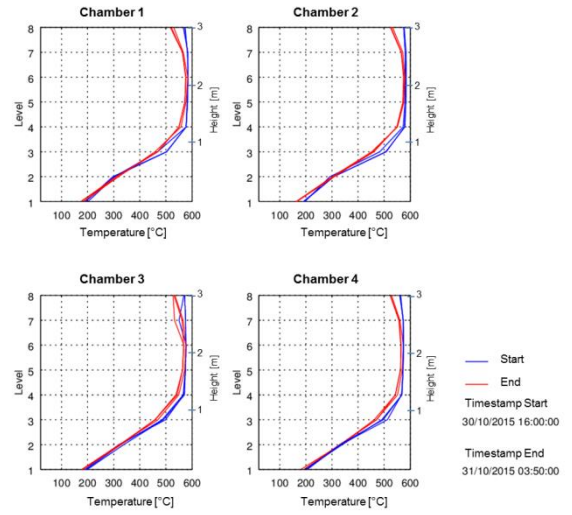**FIGURE 3.** Mean temperature of TES with damper open
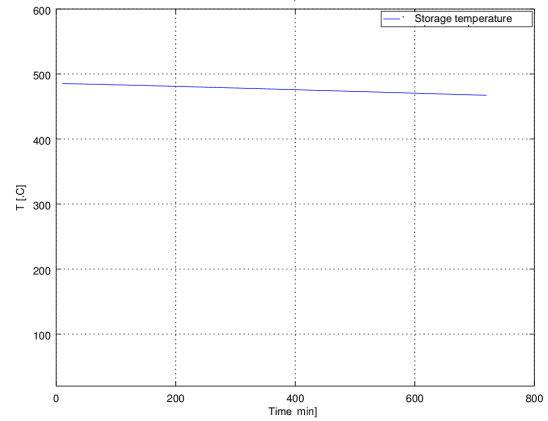
FIGURE 4. Mean temperature of TES with damper closed

It is obvious that the temperature generally decreases from start (time of shut-down of the plant) to end of the measurement, as already described above. It becomes clear that a high amount of thermal energy losses take place at the uppermost part of the storage. In the upper mid section (level 5 to 7), the temperature remains almost constant, a clear deviation is visible between level 3 and 5. In the lower levels, only very little change of temperature happens during standstill. To easily locate the areas of significant temperature change, the local temperature differences after 12 h in all chambers are plotted as contours in Fig. 7 and Fig. 8 for both cases. It becomes obvious that the highest thermal losses take place at level 8 and also the area around level 3. This indicates that a significant amount of heat from the storage gets lost to the dome and the piping connection to the storage. A drawing of the thermal energy story of the Jülich Power Tower is shown in Fig. 9. It is assumed that heat conduction through the storage and piping material causes the thermal energy loss, since the temperature gradient of the piping, which leads to the receiver, induces heat flow through the material. This in turn leads to a reallocation of isothermals inside the storage since hot air moves upwards to the top of the storage, which is why the temperature in the core of the storage chambers also decreases in some regions as the cooled region expands. The most significant peak of local temperature change is observed in chamber 2 for both cases. The effects seem to be almost independent from the damper being open or closed, which is owed to heat conduction through the piping material, although the temperature decrease is somewhat lower for the closed damper case. Due to the closed damper, the heat loss is restricted, which suggests that the total heat loss is only partially conduction but also convection. With the damper at the TES closed, more thermal energy remains in the storage.

An additional measurement has been conducted for a 56 h standstill period with the damper at the TES closed. It can be noted that the mean temperature of storage decreases almost linearly with the same cooling rate as for the 12 h case.
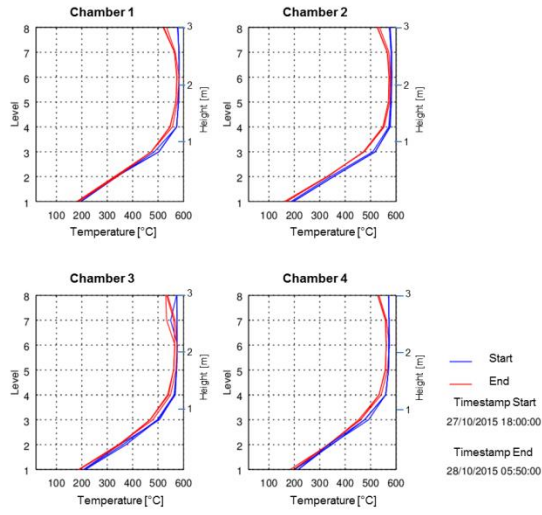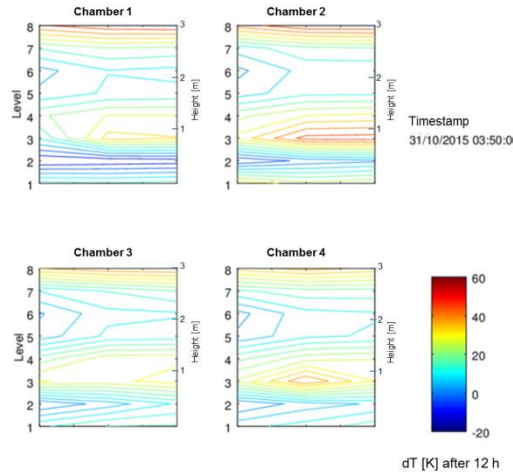
FIGURE 5. Temperature profiles of the four chambers with storage damper open at shut-down (start) and after 12 h (end)
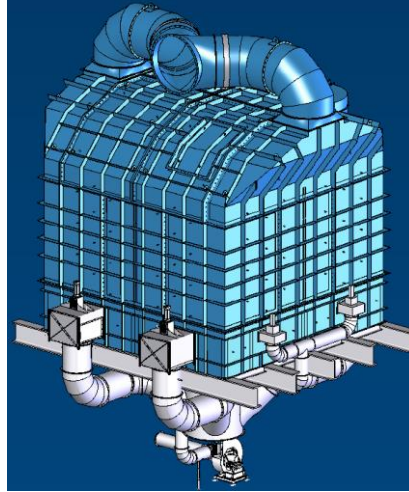

FIGURE 6. Temperature profiles of the four chambers with storage damper closed at shut-down (start) and after 12 h (end)
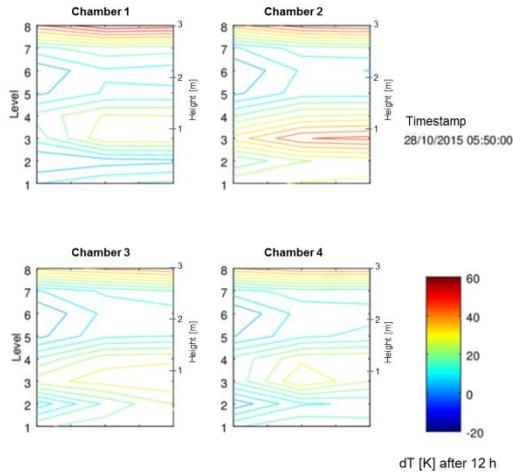
**FIGURE 7.** Isothermal lines of temperature change during downtime of 12 h with damper open

FIGURE 8. Isothermal lines of temperature change during downtime of 12 h with damper closed

**FIGURE 9**. Thermal Energy Storage of the Jülich Solar Power Tower [3]

The picture is different if only two of the four storage chambers have been charged during operation. As expected, the mean temperature is significantly reduced in comparison to the former case (175°C vs. 460°C at start of measurement). Simultaneously, the cooling rate is lower (0.67 K/h for the closed, 1,0 K/h for the open damper). This is due to the lower temperature difference to the ambient, which is much higher when the storage is fully charged. Also, there is thermal crossmixing between the hot and the cold chambers, which means that heat transfer occurs through the chamber walls from the charged to the uncharged chambers. On this account the temperature in the charged chambers decreases, the temperature in the cold chambers is almost stable and even increases during downtime if the damper is closed. The temperature profiles in the hot chambers are somewhat the same, no matter if the damper is open or closed. Fig. 10 and Fig. 11 show the mean temperature of all four chambers over time for the open and the closed damper case, respectively.
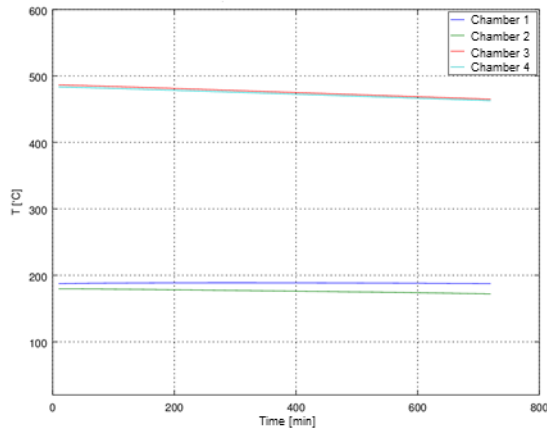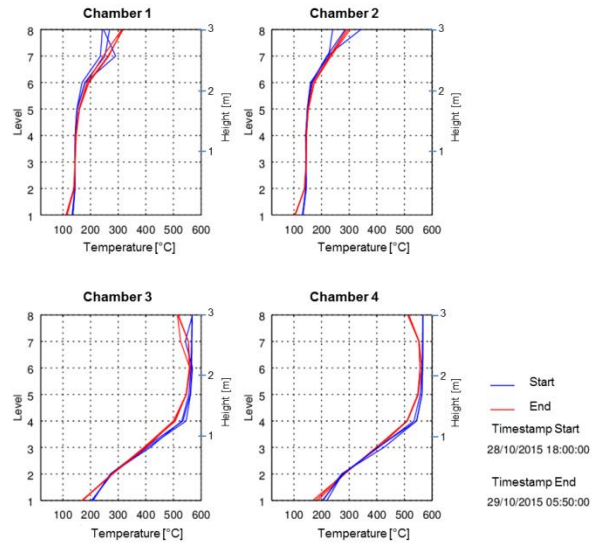

FIGURE 10. Mean temperature of all four chambers as function of downtime with storage damper open
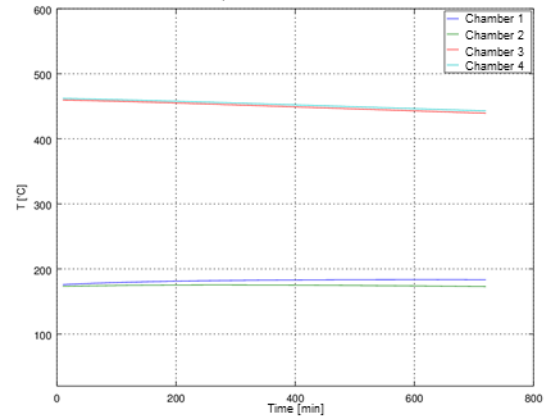
FIGURE 11. Mean temperature of all four chambers as function of downtime with storage damper closed
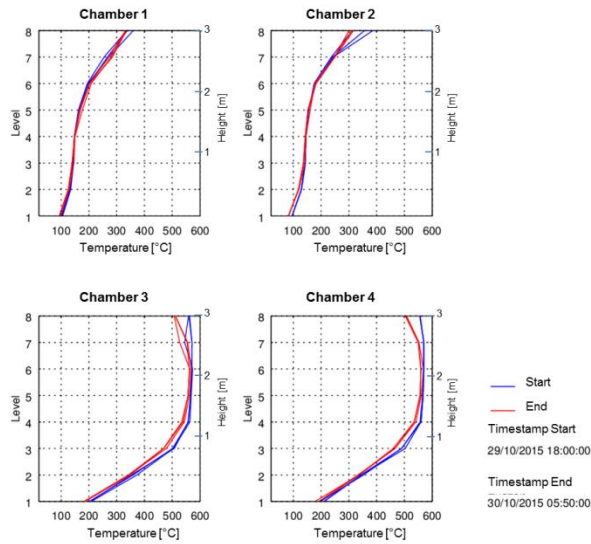
FIGURE 12. Temperature profiles of the four chambers with storage damper open, at shut-down (start) and after 12 h (end); with only chamber 1 and 2 being charged

FIGURE 13. Temperature profiles of the four chambers with storage damper closed, at shut-down (start) and after 12 h (end); with only chamber 1 and 2 being charged

As can be seen from the temperature profiles in Fig. 12 and Fig. 13, the heat exchange is very intense in the upper part of the storage. Here, the local temperatures of the cool chambers partially exceed those of the hot chambers. This suggests that inside the top of the storage, that is the dome, which is not filled with ceramic material, air convection is induced due to the temperature gradient between the chambers. Also, heat conduction through the wall between chambers contributes to the heat exchange.

With the storage partially charged and the storage damper closed, the thermal losses were reduced by 35 % compared to the case with no damper in between the receiver and the TES. Nevertheless, the total enthalpy level in this case is also reduced due to the lower temperature in two chambers. Only the two hot chambers would offer the same amount of exergy as in the fully charged case. In practice, chambers with temperatures below 200°C are useless for operating the power plant since no steam with acceptable parameters can be generated. Hence, the reduction of the usable thermal energy is only 7 % and thus comparable to the case of four charged chambers.

## Thermodynamic behavior of the steam boiler

The transient behavior of the steam boiler, which was operated at a steam pressure of 20 bar before shut-down, is shown in Fig. 14 for the open damper and in Fig. 15 for the closed damper at the boiler. The pressure represents the level of enthalpy stored in the steam. Similar to the overnight storage temperature, the steam pressure decreases almost linearly with standstill time. After nine hours, the pressure decreased by 18 %. No difference is observed whether the damper is open or closed. The rate of pressure decrease is 0.35 bar/h for both cases.

Despite the damper is closed, no reduction of thermal energy loss is achieved. This leads to the conclusion that convection in the air piping is not the primary reason for thermal losses of the system and thus negligible. The majority of heat loss to the ambient takes place via the surface of the boiler and its numerous valves and accessories, which are not or only weakly insulated for technical reasons.
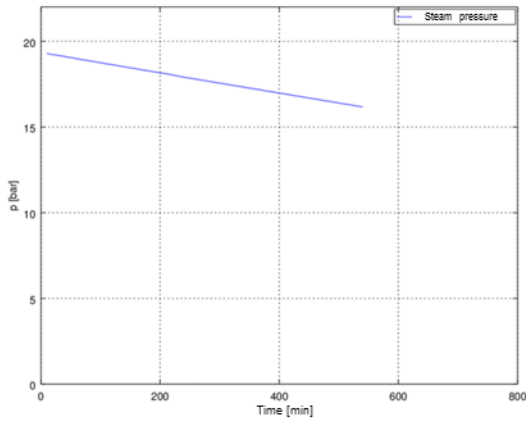
FIGURE 14. Steam pressure in the steam boiler as function of downtime with damper open
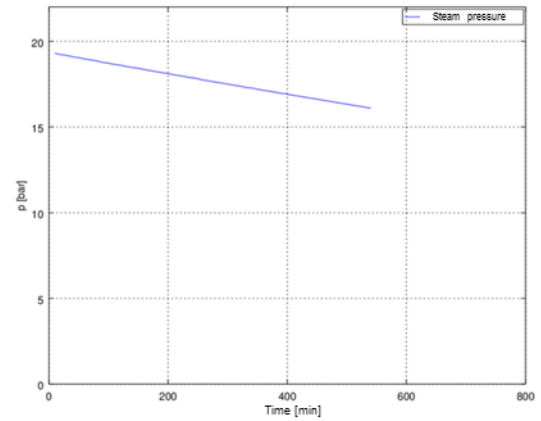
FIGURE 15. Steam pressure in the steam boiler as function of downtime with damper closed

The TES, on the other hand, is much better insulated as a whole and the inventory has a high heat capacity. Convection in the piping contributes significantly to the total heat loss of the storage.

Temperature and pressure drop at the storage-sided shut-off damper

The temperatures at both sides of the damper, the one facing the receiver and the one facing the storage, during downtime are shown in Fig. 16 and Fig. 17 with the damper open and closed, respectively. While for both cases each temperature decreases with time, the receiver-sided one decreases faster.
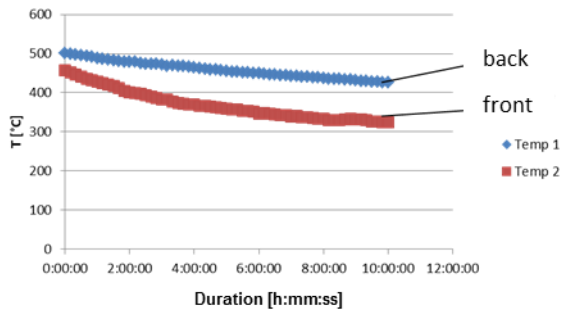
FIGURE 16. Temperatures in front (receiver-facing) and back (storage-facing) of the open storage damper as function of downtime
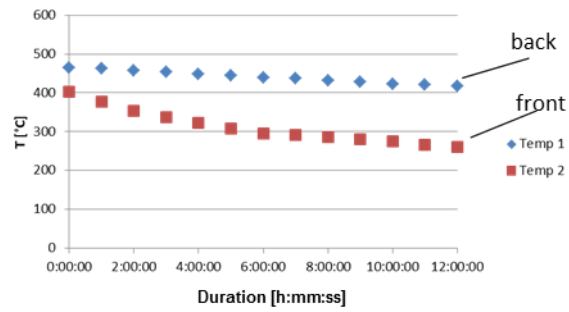
FIGURE 17. Temperatures in front (receiver-facing) and back (storage-facing) of the closed storage damper as function of downtime

The storage-facing temperature with the damper open and closed decreases by 74 K and 48 K, respectively. The difference between the two temperatures is higher for the closed damper case, while the storage-facing temperature is more stable than for the open damper case. If the damper is closed, the difference is always higher than if the damper was open. Hence, if the damper is closed, convection from the hot storage to the cooler receiver is diminished during downtime.

Pressure drop at the storage damper for different overnight configurations are shown in Fig. 18. With the damper closed, the pressure drop at shut-down is below 15 Pa. The higher pressure drop with the open damper is due to free air convection (chimney effect). The air flow in the piping induces a pressure difference at the damper.

The pressure drop decreases continuously in all cases within 12 h. This can be explained with the temperature at the receiver-facing side, which is decreasing faster than at the storage-facing side. This results in a decreasing driving temperature difference and thus, pressure drop.

Since a pressure drop also develops when the damper is closed it can be assumed that air continuously flows through the closed damper. Hence, the damper does not seal the cross section entirely and thermal energy gets lost due to convection.

Additional pressure loss measurements have been conducted during power plant operation in order to determine the pressure loss coefficient for the open dampers. The pressure loss coefficient is a parameter of each damper and can be computed applying equation 1:

$$\zeta = \frac{2\Delta p}{\rho w^2} \qquad (1)$$

Here, Δp is the measured pressure loss, ρ is the air density at current temperature, and w is the air velocity.

Air mass flows between 5 kg/s and 10 kg/s in both directions and temperatures up to 600°C were used for these measurements. The results can be found in table 2. From the results it can be seen that pressure loss, and thus the pressure loss coefficient, is a function of flow direction. In the air direction towards the storage (used for charging), the coefficient is about 1.8 times higher than for the discharge direction. The reason for this effect is that the damper leaf is not parallel to the air flow but somewhat angled and pressure loss depends on the direction of the incident flow.

It should be mentioned that within the measurement section there is a 90°-elbow installed in the piping. It is assumed the elbow contributes to the pressure loss coefficient by 0.34 (estimated according to [4]), thus this amount was subtracted from an originally computed value, in order to account for influence of the elbow in the serial chain of flow obstructions in the measurement section.
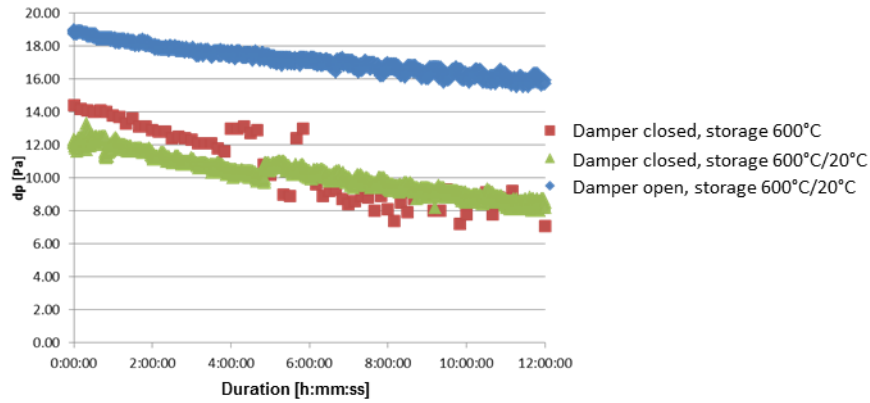

FIGURE 18. Pressure drop at the storage damper for various configurations

TABLE 2. Corrected values for the pressure loss coefficients at storage-sided and boiler-sided shut-off damper

Damper	ξ_{charge} [-]	$\xi_{discharge}$ [-]
Storage	0.81	0.29
Boiler	0.92	-

Temperature and pressure drop at the boiler-sided shut-off damper

The same investigations as for the storage damper have been conducted for the steam boiler sided damper. In Fig. 19 and Fig. 20, the temperatures at the open and the closed damper are shown, respectively. Again, the differences between the temperature in front and the back of the damper are higher for the closed damper case. Also, the declining trend over time can be found. In contrary to the storage damper, the thermal losses are significantly higher, which becomes apparent by the much lower temperatures after 10 and 12 hours, respectively. The reason for this is the lower heat storage capacity of the boiler in contrast to the storage, as well as the already discussed heat losses via the surface and external instrumentations of the boiler.
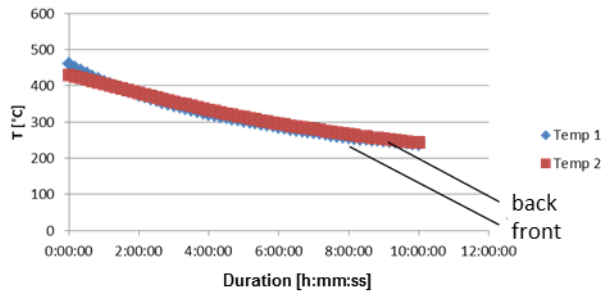
**FIGURE 19.** Temperatures in front and back of the open boiler damper
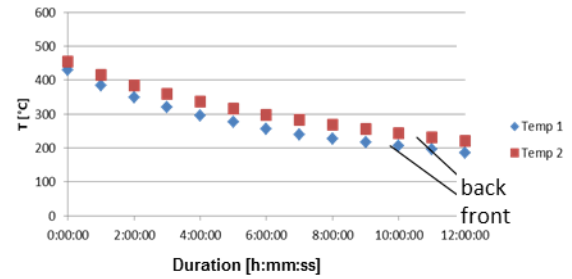
FIGURE 20. Temperatures in front and back of the open boiler damper

Also, the influence of the damper on the boiler-related heat losses are considerably lower: After 10 hours, the temperature difference between the front and the back are 37 K for the closed damper (and 5 K for the open damper). Thus, the thermal losses are reduced only marginally if the damper is closed.

In Fig. 21, the progression of pressure loss at the closed boiler damper over downtime is displayed. If the damper is closed, pressure drop drecreases from 19 Pa to 14 Pa during 12 h. As for the storage damper, it is assumed that there is an unintended leakage flow at the damper due to the chimney effect. The decrease of pressure drop over time is owed by the decreasing temperature difference between the front and the back of the damper.

As for the storage damper, the pressure loss coefficient has also been determined for the boiler damper. In contrast to the storage damper, this one can only be flowed through in one direction (from receiver to boiler). The calculated coefficient can be found in table 2. Within the measurement section, there is a complicated change of cross section which has been accounted for with a share of 0.12, which has been subtracted of an originally calculated value. The corrected value of 0.92 is somewhat higher than for the storage damper, which may result from its slightly different geometry and fitting situation (see Fig. 2).
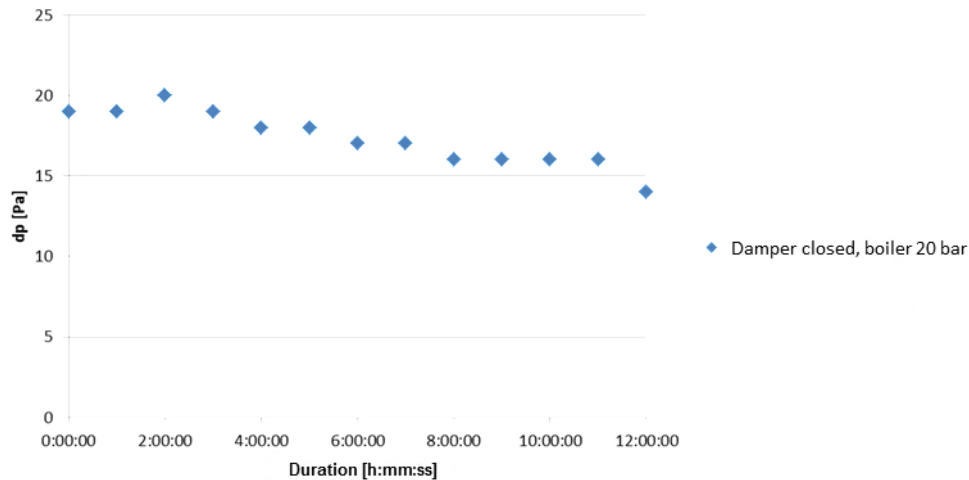
FIGURE 21. Pressure drop at the closed boiler damper

CONCLUSIONS

The investigation on the new shut-off dampers, which have been installed in the air piping system of the Juelich Solar Power Tower, showed that a reduction of thermal losses can be achieved. After the shut-off dampers have been installed, thermal losses of the fully charged thermal energy storage were reduced by about 7 % by reducing convection in the piping. At the steam boiler, no such significant reduction has been reached, which is due to the

high amount of convectional heat transfer via its surface. Here, heat losses due to the chimney effect in the piping are almost negligible.

Additionally, the dampers cannot perfectly seal the flow way (which would be technically impossible), which allows for air flow during down-time of the power plant system. Also, heat conduction through the damper leafs may induce additional heat losses. Same goes for the inventory dampers which may also account for heat losses during downtime.

The rather low efficiency of the effort indicates that natural convection in the piping is not the major thermal loss mechanism, but heat conduction in the material and heat transfer via the surfaces. With respect to the TES, the high surface area of its dome accounts for a significant amount of heat loss. These losses can be reduced applying thicker insulation layers at the appropriate locations. Future commercial CSP plants will also feature more sophisticated steam boilers which will account for lower convectional surface losses.

Although those dampers wouldn't be used on a daily basis in the first place since the storage wouldn't be fully charged overnight for normal commercial operation, they are considered useful for particular modes, e.g. if the storage should keep a certain amount of thermal energy during downtime for a quick start-up the next morning.

REFERENCES

1. S. Zunft, M. Händel, M. Krüger, V. Dreißigacker, F. Göhring, E. Wahl. Jülich Solar Power Tower—Experimental Evaluation of the Storage Subsystem and Performance Calculation, Journal of Solar Energy Engineering 133/3 (2011)
2. V. Kronhardt, S. Alexopoulos, M. Reißel, J. Sattler, B. Hoffschmidt, M. Hänel, T. Doerbeck. High-temperature thermal storage system for solar tower power plants with open-volumetric air receiver simulation and energy balancing of a discretized model, SolarPACES 2013, Energy Procedia 49 (2014)
3. KBA MetalPrint, www.kba-metalprint.com (2013)
4. W. Wagner, Strömung und Druckverlust, Vogel Buchverlag, 7th edition (2012)